Supplemental Material for "Symmetry breaking and error correction in open quantum systems"

Simon Lieu,[1,2] Ron Belyansky,[1,2] Jeremy T. Young,[1] Rex Lundgren,[1,2] Victor V. Albert,[3,4] Alexey V. Gorshkov[1,2]

[1] *Joint Quantum Institute, NIST/University of Maryland, College Park, MD 20742, USA*
[2] *Joint Center for Quantum Information and Computer Science, NIST/University of Maryland, College Park, Maryland 20742 USA*
[3] *Institute for Quantum Information and Matter and Walter Burke Institute for Theoretical Physics, California Institute of Technology, Pasadena, CA 91125, USA*
[4] *National Institute of Standards and Technology, Gaithersburg, MD 20899, USA*

In Sec. 1, we analytically show that the dissipative gap closes at the critical point by utilizing an exact solution for the Lindblad spectrum [Fig. 1(b) in the main text]. Sec. 2 exhibits numerical evidence for a noiseless subsystem steady state in the strong-broken phase (away from $\mathcal{L}_0$). Sec. 3 tracks the evolution of the state throughout the error protocol in the main text. We show numerical evidence for the state structure defined in Eq. (5) of the main text for errors which keep the model in the strong-broken phase. Sec. 4 uses the asymptotic projection method to confirm perfect fidelity recovery in the thermodynamic limit, in agreement with the direct numerical evolution discussed in the main text. In Sec. 5 we show that a *classical bit* encoded into the steady state is protected against perturbations which keep the Lindbladian in the *weak-broken* phase.

1. CLOSING OF THE DISSIPATIVE GAP AT THE CRITICAL POINT

We show that an extensive number of spectral eigenvalues touch zero at the critical boundary [Fig. 1(a) in the main text] when approaching from the unbroken phase in the thermodynamic limit. We utilize Prosen's "third quantization" technique which allows us to fully diagonalize a quadratic Lindbladian [S1, S2]. For the Hamiltonian (3) in the presence of one-photon loss only (i.e. the weak transition), the Lindbladian can be expressed as $\mathcal{L} = \epsilon_+ \beta_+^\dagger \beta'_+ + \epsilon_- \beta_-^\dagger \beta'_-$, where β are bosonic superoperators satisfying generalized commutation relations $[\beta'_i, \beta_j^\dagger] = \delta_{ij}$. These excite a quantum of "complex energy" $\epsilon_\pm = -\kappa_1 \pm \sqrt{4\lambda^2 - \omega^2}$, where the (unique) steady state is annihilated by all quasiparticles $\beta'_\pm \rho_{ss} = 0$, and the many-body spectrum is built from these single-particle excitations $\mathcal{L}[(\beta_+^\dagger)^n (\beta_-^\dagger)^m \rho_{ss}] = (n\epsilon_+ + m\epsilon_-)[(\beta_+^\dagger)^n (\beta_-^\dagger)^m \rho_{ss}]$. The single-particle spectrum touches zero at $\kappa_1/\omega = \sqrt{4(\lambda/\omega)^2 - 1}$, which coincides with the emergence of a non-zero order parameter (see main text). This implies that an infinite number of eigenvalues of $\mathcal{L}$ are zero at the critical point of the weak transition from 1 steady state to 2 steady states. We plot both the single-particle spectrum and match it with many-body numerics in Fig. S1. [Fig. S1(a) and Fig. 1(b) are equivalent; here we plot the real and imaginary parts side by side.] The numerical spectrum deviates from analytical predictions only near the critical boundary due to truncation of the Hilbert space dimension. Note that the analytical and numerical plots are only valid in the unbroken phase. The steady state has an infinite number of photons in the broken phase, hence any finite-size Hilbert space will not produce a converged spectrum. Finite-size scaling [Fig. 1(d)] suggests that two eigenvalues are exponentially close to zero in the weak-broken phase with a dissipative gap to the rest of the modes.

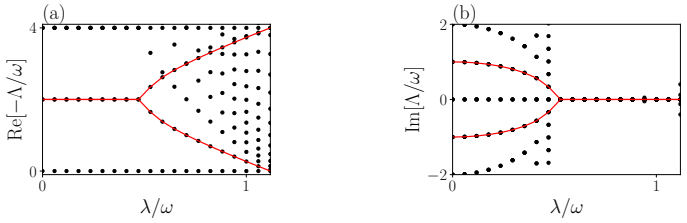

FIG. S1. Analytical single-particle spectrum (red lines) and numerical many-body spectrum (black dots) with $\kappa_1/\omega = 2, \kappa_2 = \kappa_d = 0$. The many-body spectrum comes in integer multiples of the single-particle excitations. As the system approaches the critical point from the unbroken phase, the single-particle spectrum touches zero at the phase boundary $\lambda/\omega \approx 1.1$. The numerical spectrum starts to deviate from the analytical predictions near the transition due to truncation of the Hilbert space dimension $d_{\text{Hilbert}} = 70$. We plot up to 25 eigenvalues closest to zero for clarity.

2. NOISELESS SUBSYSTEM IN THE STRONG-BROKEN PHASE

We demonstrate that the model described in the main text possesses a qubit steady-state structure in the thermodynamic limit of the strong-broken phase. In particular, we will show that the four right eigenoperators with zero eigenvalue can be written in the form $r_{\mu\nu} = |\mu\rangle\langle\nu| \otimes z$ with $(\mu, \nu) \in (+, -)$. This is called a noiseless subsystem (NS) if z is mixed, and a decoherence-free subspace (DFS) if z is pure [S3–S5].

The four steady-state right eigenoperators belonging to the different parity sectors are

$$r^F_{++} = \begin{pmatrix} s_{++} & 0 \\ 0 & 0 \end{pmatrix}, \qquad r^F_{--} = \begin{pmatrix} 0 & 0 \\ 0 & s_{--} \end{pmatrix}, \qquad r^F_{+-} = \begin{pmatrix} 0 & s_{+-} \\ 0 & 0 \end{pmatrix}, \qquad r^F_{-+} = \begin{pmatrix} 0 & 0 \\ s_{-+} & 0 \end{pmatrix} \tag{S1}$$

in the Fock basis $[|0\rangle, |2\rangle, |4\rangle, \ldots, |1\rangle, |3\rangle, |5\rangle, \ldots]^T$. They each satisfy $\mathcal{L}(r) = 0$ (in the thermodynamic limit). Since s_{++}, s_{--} are guaranteed to be Hermitian matrices, we can diagonalize them via a unitary transformation $U = \mathrm{Diag}[U_+, U_-]$ which relates the Fock basis to the diagonal basis $r^d_i = U^\dagger r^F_i U$. In this new basis, the eigenoperators are

$$r^d_{++} = \begin{pmatrix} z_{++} & 0 \\ 0 & 0 \end{pmatrix}, \qquad r^d_{--} = \begin{pmatrix} 0 & 0 \\ 0 & z_{--} \end{pmatrix}, \qquad r^d_{+-} = \begin{pmatrix} 0 & z_{+-} \\ 0 & 0 \end{pmatrix}, \qquad r^d_{-+} = \begin{pmatrix} 0 & 0 \\ z_{-+} & 0 \end{pmatrix}, \tag{S2}$$

where z_{++}, z_{--} are diagonal by construction, and z_{+-}, z_{-+} are diagonal in the thermodynamic limit. We will show that $z_{++} = z_{--} = z_{+-} = z_{-+}$ in this limit, which implies that the system hosts a NS or a DFS.

In the special limit $\omega = \kappa_d = \kappa_1 = 0, \lambda \neq 0, \kappa_2 \neq 0$, any pure superposition of even and odd cat states remains steady, as discussed in the main text. Thus $z_{++} = z_{--} = z_{+-} = z_{-+} = \mathrm{Diag}[1, 0, 0, 0, \ldots]$, which implies a DFS.

We now consider a parameter regime away from this limit but within the strong-broken phase. We start by adding dephasing: $\omega = \kappa_1 = 0, \kappa_d \neq 0, \lambda \neq 0, \kappa_2 \neq 0$. We will numerically show that the z matrices are equal and not pure. For the matrix distance, we choose the trace distance $D_t(A, B) = \mathrm{Tr}[\sqrt{(A-B)^2}]/2$. In Fig. S2(a,b), we plot $D_t(z_{++}, z_{--})$ and $D_t(z_{++}, z_{+-})$ as the system approaches the thermodynamic limit $\lambda/\kappa_2 = N \to \infty$. Indeed, we find that the matrices z_{++}, z_{--}, z_{+-} all converge to a single matrix as N is increased. (z_{+-} and z_{-+} are related by Hermiticity.) Additionally, in Fig. S2(c), we show that z_{++} is a non-pure matrix with elements that fall off as $(z_{++})_{ii} \sim \exp[-i]$. The purity of z_{++} *degrades* with N (not shown). We conclude that the system tends to a noiseless subsystem in the thermodynamic limit, since the $z_{\pm\pm}$ all converge to a single non-pure matrix. [For completeness, in Fig. S2(d), we show that the smallest eigenvalue in the off-diagonal sector indeed tends to zero exponentially quickly with N. The steady-state degeneracy is split by an exponentially small factor, characteristic of symmetry-breaking transitions.]

We repeat this analysis in the limit of no dephasing but non-zero ω: $\kappa_d = \kappa_1 = 0, \omega \neq 0, \lambda \neq 0, \kappa_2 \neq 0$. Fig. S3 shows that the $z_{\pm\pm}$ converge to a single non-pure matrix in the thermodynamic limit, similar to the case of dephasing. We therefore conclude that a generic model in the strong-broken phase possesses a noiseless subsystem, whilst a decoherence-free subspace exists at a special point $\mathcal{L}_0$ in the phase diagram.

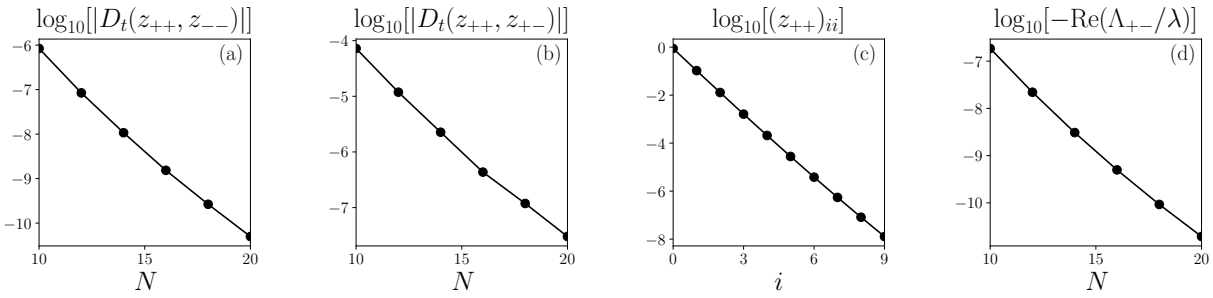

FIG. S2. Parameters: $\lambda/\kappa_2 = N, \kappa_d/\lambda = 0.03, \omega = \kappa_1 = 0$, i.e. non-zero dephasing. (a,b) The trace norm $D_t(A, B) = \mathrm{Tr}[\sqrt{(A-B)^2}]/2$ between the different right eigenoperators with zero eigenvalue goes to zero in the thermodynamic limit $N \to \infty$. (c) Diagonal matrix elements of z_{++} for $N = 20$. The matrix is not pure, with elements scaling as $(z_{++})_{ii} \sim \exp[-ci]$ for some $c > 0$. (d) The off-diagonal symmetry sector of the Lindbladian acquires an eigenvalue of zero as $N \to \infty$. Here Λ_{+-} is the smallest eigenvalue in the off-diagonal sector.

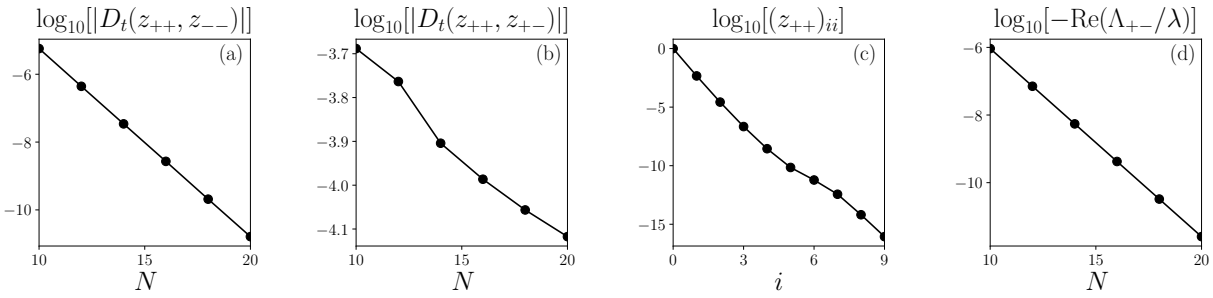

FIG. S3. Parameters: $\lambda/\kappa_2 = N, \omega/\lambda = 0.5, \kappa_d = \kappa_1 = 0$. (a,b) The trace norm between the different right eigenoperators with zero eigenvalue goes to zero in the thermodynamic limit $N \to \infty$. (c) Diagonal matrix elements of z_{++} for $N = 20$. The matrix is not pure, with elements scaling as $(z_{++})_{ii} \sim \exp[-ci]$ for some $c > 0$. (d) The off-diagonal symmetry sector of the Lindbladian acquires an eigenvalue of zero as $N \to \infty$. Here Λ_{+-} is the smallest eigenvalue in the off-diagonal sector.

3. EVOLUTION FROM DECOHERENCE-FREE SUBSPACE TO NOISELESS SUBSYSTEM

We now track the state throughout the error protocol described in the main text for both dephasing errors and Hamiltonian-frequency errors. Our analysis will confirm that the state can be written as a qubit tensored with a mixed state thoughout the entire quench protocol, i.e. the structure described in Eq. (5) in the main text. An analytical understanding of this mechanism requires an exact solution for the steady states in the entire strong-broken phase—an important direction for future work.

We prepare the system in a pure steady state of $\mathcal{L}_0$:

$$\rho_i = \begin{pmatrix} |c_e|^2 & c_e c_o^* \\ c_e^* c_o & |c_o|^2 \end{pmatrix} \tag{S3}$$

in the basis of even and odd cat states $|\alpha\rangle_e, |\alpha\rangle_o$, where $|c_e|^2 + |c_o|^2 = 1$ and $\mathcal{L}_0(\rho_i) = 0$. We evolve this initial state with an error to a "middle" state

$$\rho_m(\tau_q) = e^{(\mathcal{L}_0 + \mathcal{L}')\tau_q} \rho_i. \tag{S4}$$

We wish to show that this middle state can be written in the form

$$\rho_m(\tau_q) = \begin{pmatrix} |c_e|^2 & c_e c_o^* \\ c_e^* c_o & |c_o|^2 \end{pmatrix} \otimes M \tag{S5}$$

for some M which is not necessarily pure.

We numerically solve for $\rho_m(\tau_q)$ via Eq. (S4) for arbitrary quench times and $\mathcal{L}_0 + \mathcal{L}'$ in the strong-broken phase. We then split the matrix up into symmetry sectors in the Fock basis $\rho_m = |c_e|^2 \rho^F_{++} + |c_o|^2 \rho^F_{--} + (c_e c_o^* \rho^F_{+-} + h.c.)$. The four operators belonging to the different parity sectors are

$$\rho^F_{++} = \begin{pmatrix} x_{++} & 0 \\ 0 & 0 \end{pmatrix}, \quad \rho^F_{--} = \begin{pmatrix} 0 & 0 \\ 0 & x_{--} \end{pmatrix}, \quad \rho^F_{+-} = \begin{pmatrix} 0 & x_{+-} \\ 0 & 0 \end{pmatrix}, \quad \rho^F_{-+} = \begin{pmatrix} 0 & 0 \\ x_{-+} & 0 \end{pmatrix} \tag{S6}$$

in the Fock basis $[|0\rangle, |2\rangle, |4\rangle, \ldots, |1\rangle, |3\rangle, |5\rangle, \ldots]^T$. Since x_{++}, x_{--} are guaranteed to be Hermitian matrices, we can diagonalize them via a unitary transformation $V = \mathrm{Diag}[V_+, V_-]$ which relates the Fock basis to the diagonal basis $\rho^d_i = V^\dagger \rho^F_i V$. In this new basis, the eigenoperators are

$$\rho^d_{++} = \begin{pmatrix} M_{++} & 0 \\ 0 & 0 \end{pmatrix}, \quad \rho^d_{--} = \begin{pmatrix} 0 & 0 \\ 0 & M_{--} \end{pmatrix}, \quad \rho^d_{+-} = \begin{pmatrix} 0 & M_{+-} \\ 0 & 0 \end{pmatrix}, \quad \rho^d_{-+} = \begin{pmatrix} 0 & 0 \\ M_{-+} & 0 \end{pmatrix}, \tag{S7}$$

where all the Ms are diagonal by construction. We now show that all Ms converge to a single matrix in the thermodynamic limit, confirming the form of Eq. (S5).

We plot the trace distance between the different Ms for both short and long quench times $\tau_q \lambda \in [10^{-2}, 10^2]$. In Fig. S4, we consider a quench in the dephasing strength. Indeed, the trace distance between the different Ms goes to zero exponentially fast as a function of N, which suggests that the ansatz in Eq. (S5) is correct in the limit $N \to \infty$.

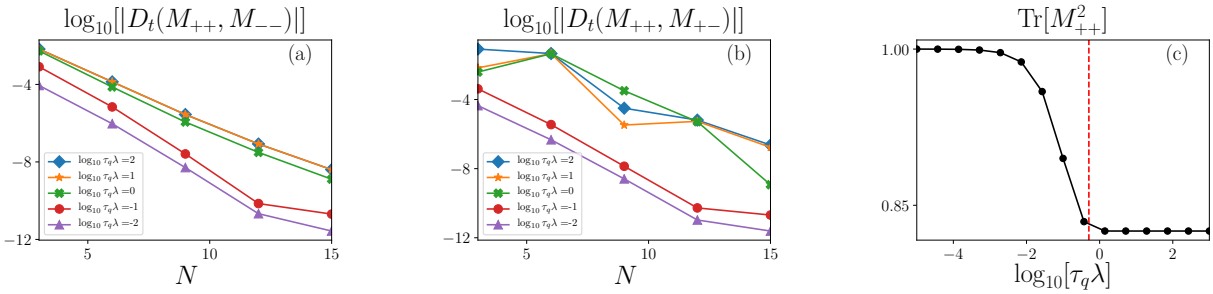

FIG. S4. Parameters: $\lambda/\kappa_2 = N, \kappa_d/\lambda = 0.03, \omega = \kappa_1 = 0, c_e = 1/\sqrt{2}, c_o = i/\sqrt{2}$. (a) The trace distance between M_{++} and M_{--} goes to zero exponentially fast in N. (b) Analogous behavior is observed for M_{++} and M_{+-}. (c) $N = 15$, the red line is the time scale set by the inverse dissipative gap $\tau_g = \Delta_g^{-1}$ of $\mathcal{L}_0 + \mathcal{L}'$. The state is approximately pure for short quenches compared to this time scale, while it settles to its (mixed) steady-state value for quenches longer than this timescale.

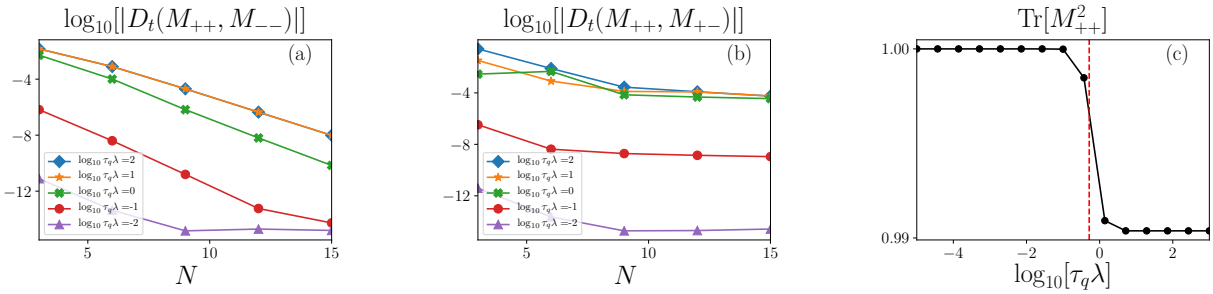

FIG. S5. Parameters: $\lambda/\kappa_2 = N, \omega/\lambda = 0.5, \kappa_d = \kappa_1 = 0, c_e = 1/\sqrt{2}, c_o = i/\sqrt{2}$. (a) The trace distance between M_{++} and M_{--} goes to zero exponentially fast in N. (b) Analogous behavior is observed for M_{++} and M_{+-}. (c) $N = 15$, the red line is the time scale set by the inverse dissipative gap $\tau_g = \Delta_g^{-1}$ of $\mathcal{L}_0 + \mathcal{L}'$. The state is approximately pure for short quenches compared to this time scale, while it settles to its (mixed) steady-state value for quenches longer than this timescale.

We also track the purity of this matrix: At quench times that are short compared to the timescale set by the dissipative gap (red line), the middle state remains approximately pure, whilst longer quenches imply that the system settles into its new steady state, which is mixed (see previous section). Analogous behavior is observed for a quench in frequency (Fig. S5).

4. ASYMPTOTIC PROJECTION

We verify the perfect recovery of the fidelity observed in Fig. 2 of the main text via the asymptotic projection method [S6]. Fig. 2 shows that qubit cat states will self correct via the environment if $\mathcal{L}_0 + \mathcal{L}'$ remains in the strong symmetry-broken phase. This behavior can be understood via perturbation theory for short quenches (compared to the time scale set by the dissipative gap) [S7]. Here, we consider long quench times where the system evolves into the steady state of $\mathcal{L}_0 + \mathcal{L}'$. Remarkably, such a drastic error can still be passively corrected via the environment $\mathcal{L}_0$. We provide simple expressions relating the initial, intermediate, and final states by projecting onto the corresponding steady state manifolds.

Defining our initial state as ρ_i, we evolve it with an error $(\mathcal{L}_0 + \mathcal{L}')$ to a "middle" state $\rho_m(\tau_q) = e^{(\mathcal{L}_0+\mathcal{L}')\tau_q}\rho_i$. We then evolve the state with $\mathcal{L}_0$ for an infinite time to reach the final state $\rho_f(\tau_q) = \lim_{\tau\to\infty} e^{\mathcal{L}_0\tau}\rho_m(\tau_q)$. We will discuss how $\rho_{i,m,f}$ relate to one another in this protocol when τ_q is much longer than the inverse dissipative gap of $\mathcal{L}_0 + \mathcal{L}'$.

We first prepare the system in a pure steady state of $\mathcal{L}_0$,

$$\rho_i = |a|^2 r^0_{++} + |b|^2 r^0_{--} + a^* b r^0_{+-} + a b^* r^0_{-+}, \tag{S8}$$

where $r^0_{++} = |\alpha\rangle_e \langle\alpha|_e$, $r^0_{--} = |\alpha\rangle_o \langle\alpha|_o$, $r^0_{+-} = |\alpha\rangle_e \langle\alpha|_o$, $r^0_{-+} = |\alpha\rangle_o \langle\alpha|_e$; $|\alpha\rangle_{e/o}$ is the even/odd cat state, and $\mathcal{L}_0(r^0_{\pm\pm}) = 0$. To find ρ_m, it is useful to define the right and left eigenoperators of the error:

$$(\mathcal{L}_0 + \mathcal{L}')(\tilde{r}_j) = \tilde{\Lambda}_j(\tilde{r}_j), \qquad (\mathcal{L}_0^\dagger + \mathcal{L}'^\dagger)(\tilde{l}_j) = \tilde{\Lambda}_j^*(\tilde{l}_j), \tag{S9}$$

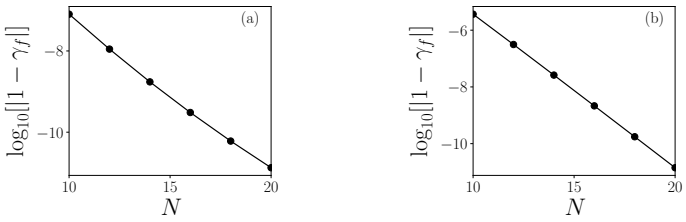

FIG. S6. Scaling of $|1-\gamma_f|$ as a function of N for (a) a dephasing error $\lambda/\kappa_2 = N, \kappa_d/\lambda = 0.03$ and (b) a frequency error $\lambda/\kappa_2 = N, \omega/\lambda = 0.03$. γ_f approaches one exponentially fast in N for both cases.

where the spectrum $\{\tilde{\Lambda}\}$ and eigenoperators determine the dynamics under $\mathcal{L}_0 + \mathcal{L}'$. Assuming that the error keeps the system in the strong-broken phase, we know that two eigenvalues will be exactly zero $\tilde{\Lambda}^0_{++} = \tilde{\Lambda}^0_{--} = 0$ and two eigenvalues will be exponentially close to zero $\tilde{\Lambda}^0_{+-} = (\tilde{\Lambda}^0_{-+})^* \sim e^{-N}$. We label the eigenvalue of the first "excited" state (above these four) as $\tilde{\Lambda}_g$, which sets the dissipative gap in the thermodynamic limit. The exact expression for $\rho_m(\tau_q)$ reads

$$\rho_m(\tau_q) = \sum_j \exp[\tilde{\Lambda}_j \tau_q] \mathrm{Tr}[\tilde{l}_j^\dagger \rho_i] \tilde{r}_j, \tag{S10}$$

where we have used the orthogonality relation $\mathrm{Tr}[\tilde{l}_j^\dagger \tilde{r}_k] = \delta_{jk}$. $-\mathrm{Re}[\tilde{\Lambda}_j^{-1}]$ sets the lifetime of each eigenoperator. Consider a quench time that obeys $-\mathrm{Re}[\tilde{\Lambda}_g^{-1}] \ll \tau_q \ll -\mathrm{Re}[(\tilde{\Lambda}^0_{+-})^{-1}] \sim e^N$. This quench is long enough for the system to relax into the new steady state but not so long that coherences are lost. In this regime, ρ_m will tend to the following matrix t_m

$$\lim_{N\to\infty} \rho_m(\tau_q) = t_m, \qquad t_m = |a|^2 \tilde{r}^0_{++} + |b|^2 \tilde{r}^0_{--} + \left[a^* b \gamma_m \tilde{r}^0_{+-} + h.c.\right], \qquad \gamma_m = \mathrm{Tr}\left[(\tilde{l}^0_{+-})^\dagger r^0_{+-}\right]. \tag{S11}$$

If τ_q is longer than $-\mathrm{Re}[\tilde{\Lambda}_g^{-1}]$, then all excitations will vanish and we will be left with the projection onto the steady-state manifold of the error. We have confirmed this numerically by doing the full time evolution $\rho_m = \exp\left[(\mathcal{L}+\mathcal{L}')\tau_q\right]\rho_i$ and comparing the resulting matrix with t_m. Indeed, the trace distance $D_t(\rho_m, t_m) = \mathrm{Tr}[\sqrt{(\rho_m - t_m)^2}]/2)$ goes to zero exponentially quickly in N. We have thus found a simple expression for $\rho_m(\tau_q)$ for this range of τ_q.

Having understood the structure of this intermediate state, $\rho_m \approx t_m$, we now project this state back onto the steady-state manifold of $\mathcal{L}_0$. Without any additional approximations, the resulting state is

$$\lim_{N\to\infty} \rho_f = |a|^2 r^0_{++} + |b|^2 r^0_{--} + \gamma_f a^* b r^0_{+-} + \gamma_f^* a b^* r^0_{-+}, \qquad \gamma_f = \mathrm{Tr}[(\tilde{l}^0_{+-})^\dagger r^0_{+-}]\mathrm{Tr}[(l^0_{+-})^\dagger \tilde{r}^0_{+-}]. \tag{S12}$$

We see that the final state is very simply related to the initial state via the γ_f parameter in Eq. (S12). Moreover, numerically we observe that γ_f approaches 1 exponentially fast in the thermodynamic limit, depicted in Fig. S6 for both the case of (a) $\kappa_d \neq 0$ and (b) $\omega \neq 0$. (We have also checked that γ_m approaches 1 in the same limit.) This implies that the final state ρ_f is indeed expected to return to its initial (pure) state ρ_i in the thermodynamic limit.

Structure of the left eigenoperators $\tilde{l}$

In Sec. 3 and earlier in this Section, we saw that the initial state settles into the noiseless subsystem of the intermediate Lindbladian $\mathcal{L}_0 + \mathcal{L}'$ without losing any coherences as $N \to \infty$. We would like to find a simple explanation for this behavior. This evolution would be accounted for (in the limit $N \to \infty$) if the left eigenoperators of $\mathcal{L}_0 + \mathcal{L}'$ with zero eigenvalue are equal to the identity in each symmetry sector, since, in this case, $\gamma_m = \mathrm{Tr}[(l^0_{+-})^\dagger \tilde{r}^0_{+-}] = \mathrm{Tr}[\tilde{s}^0_{+-}] = \mathrm{Tr}[\tilde{z}^0_{+-}] = 1$ where in the last step we have used $\mathrm{Tr}[\tilde{z}^0_{+-}] = \mathrm{Tr}[\tilde{z}^0_{++}] = 1$. (See Sec. 2 for definitions of r, s, z.) We will show that this is indeed true. Splitting up the left eigenoperators into symmetry sectors, we have

$$\tilde{l}^F_{++} = \begin{pmatrix} y_{++} & 0 \\ 0 & 0 \end{pmatrix}, \qquad \tilde{l}^F_{--} = \begin{pmatrix} 0 & 0 \\ 0 & y_{--} \end{pmatrix}, \qquad \tilde{l}^F_{+-} = \begin{pmatrix} 0 & y_{+-} \\ 0 & 0 \end{pmatrix}, \qquad \tilde{l}^F_{-+} = \begin{pmatrix} 0 & 0 \\ y_{-+} & 0 \end{pmatrix}. \tag{S13}$$

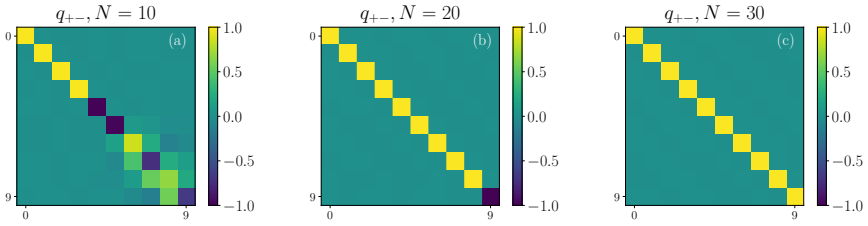

FIG. S7. Plot of a 10×10 block of q_{+-}; all elements are real. Parameters: $\kappa_2/\lambda = 1/N, \kappa_d/\lambda = 0.03, \omega = \kappa_1 = 0$. As the system approaches the thermodynamic limit, the matrix tends to the identity.

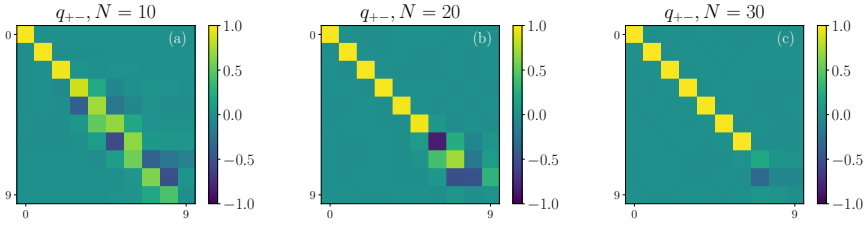

FIG. S8. Plot of a 10×10 block of q_{+-}; all elements are real. Parameters: $\kappa_2/\lambda = 1/N, \omega/\lambda = 0.5, \kappa_d = \kappa_1 = 0$. As the system approaches the thermodynamic limit, the matrix tends to the identity.

As before, we are in the Fock basis $[|0\rangle, |2\rangle, |4\rangle, \ldots, |1\rangle, |3\rangle, |5\rangle, \ldots]^T$. Then $y_{++} = y_{--} = \mathbb{I}$ since any arbitrary initial state must have unit overlap with the steady-state solutions with non-zero trace. Now we switch from the Fock basis to the diagonal basis of r, $r_i^d = U^\dagger r_i^F U$, $\tilde{l}_i^d = U^\dagger \tilde{l}_i^F U$, and obtain

$$\tilde{l}_{++}^d = \begin{pmatrix} q_{++} & 0 \\ 0 & 0 \end{pmatrix}, \qquad \tilde{l}_{--}^d = \begin{pmatrix} 0 & 0 \\ 0 & q_{--} \end{pmatrix}, \qquad \tilde{l}_{+-}^d = \begin{pmatrix} 0 & q_{+-} \\ 0 & 0 \end{pmatrix}, \qquad \tilde{l}_{-+}^d = \begin{pmatrix} 0 & 0 \\ q_{-+} & 0 \end{pmatrix}. \tag{S14}$$

Again, $q_{++} = q_{--} = \mathbb{I}$; we shall now probe the structure of the off-diagonal matrix q_{+-}.

In this basis, the four *right* eigenoperators r of $\mathcal{L}_0 + \mathcal{L}'$ with zero eigenvalue are just a single diagonal matrix z in each of the four symmetry quadrants in the thermodynamic limit (see Sec. 2). This matrix z is not pure, and in principle has infinite rank although its eigenvalues fall off exponentially quickly as a function of the index, i.e. $z_{jj} \sim e^{-cj}$ for some $c > 0$. In the case of a noiseless subsystem with full rank z, Ref. [S8] proved that the corresponding conserved quantity must be the identity in each symmetry sector for a finite-dimensional Hilbert space. Since our bosonic model has an infinite-dimensional Hilbert space, these results do not immediately apply. Nevertheless, we numerically show that the conserved quantities approach the identity in the thermodynamic limit.

In Fig. S7, we plot the elements of a 10×10 block of the matrix q_{+-} for the case of non-zero dephasing. Indeed, we find that the matrix tends to the identity as we approach the thermodynamic limit. The matrix q_{+-} acquires off-diagonal terms at entries where the corresponding matrix elements z'_{jj} are small, i.e. we are limited by numerical precision. Analogous behavior is observed for the case of non-zero ω, depicted in Fig. S8. So indeed we expect $\lim_{N\to\infty} q_{+-} = \mathbb{I}$ for the full rank noiseless subsystem. This explains why ρ_i does not lose coherences when relaxing into the steady state of $\mathcal{L}_0 + \mathcal{L}'$.

5. PASSIVE PROTECTION OF A CLASSICAL BIT IN THE WEAK-BROKEN PHASE

Up to now, we have focused on describing the quantum error correcting properties for a qubit encoded in the steady state of $\mathcal{L}_0$ subject to errors that keep it in the *strong-broken* phase. Here, we show that a classical bit encoded into the steady state of $\mathcal{L}_0$ will be passively protected against any error which keeps the model in the *weak-broken* phase. This region of parameter space includes single-photon loss, which is non-negligible in experimental setups and represents the dominant decoherence mechanism for photonic cat qubits.

We consider the same protocol as in the main text, but with a restricted initial state: Initialize the system in the state $\rho_i = c|\alpha\rangle\langle\alpha| + (1-c)|-\alpha\rangle\langle-\alpha|$ where $c = 0$ or 1, which represents the classical bit and satisfies $\mathcal{L}_0(\rho_i) = 0$. (Any choice of $c \in [0, 1]$ will also exhibit protection.) Then quench the state with an "error" for an arbitrary time τ_q to obtain $\rho_m = \exp[(\mathcal{L}_0 + \mathcal{L}')\tau_q](\rho_i)$. Finally, turn off the error and evolve the system with $\mathcal{L}_0$ for a long time such

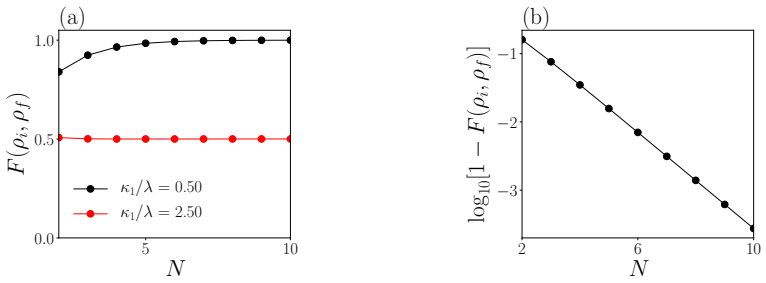

FIG. S9. Fidelity of the initial and final *classical*-bit state with $c = 1, \lambda/\kappa_2 = N, \kappa_d = \omega = 0, \tau_q\lambda = 10$, $F(\rho_i, \rho_f) = \mathrm{Tr}[\sqrt{\sqrt{\rho_i}\rho_f\sqrt{\rho_i}}]^2$. Quenches to the weak-broken phase (black dots) have a fidelity that tends to one in the thermodynamic limit, while quenches to the weak-unbroken phase (red dots) do not. (b) Same parameters as in (a) with $\kappa_1/\lambda = 0.5$; the fidelity tends to one exponentially fast in N.

that it reaches its steady state: $\rho_f = \lim_{t\to\infty} \exp[\mathcal{L}_0 t](\rho_m)$. We show that any error which keeps the model in the *weak-broken* phase is correctable passively.

In Fig. S9, we plot the fidelity between the initial and final states after a long quench of single-photon-loss error $L_1' = \sqrt{\kappa_1}a$. Only if the error keeps the model in the weak-broken phase (i.e. $\kappa_1/\lambda < 2$) does the classical bit recover its initial state in the thermodynamic limit.

We can understand this behavior by considering the steady-state structure for a generic system in the weak-broken phase. In a parity basis, it assumes the form

$$\rho_{ss} = \begin{pmatrix} 1/2 & c - 1/2 \\ c - 1/2 & 1/2 \end{pmatrix} \otimes z, \tag{S15}$$

where $c \in [0, 1]$ is a real variable parameterizing the classical-bit manifold, and z is some (generically mixed) state. This structure is in agreement with Table 2 in the main text. This suggests that any time after the introduction of the error, the state has the form

$$\rho_m(\tau_q) = \begin{pmatrix} 1/2 & c - 1/2 \\ c - 1/2 & 1/2 \end{pmatrix} \otimes M(\tau_q) \ , \tag{S16}$$

where the classical bit c remain perfectly stored in the off-diagonal sector and only M changes. If the error is large enough to move the system to the weak-unbroken phase (e.g. $\kappa_1/\lambda > 2$), then the state will evolve toward a unique steady state and the classical information will be lost. This agrees with our numerical results.

Going back to cat qubit superpositions encoded in the steady state of $\mathcal{L}_0$, *i.e.*, $|\psi\rangle = c_1|\alpha\rangle + c_0|-\alpha\rangle$, our analysis implies that "small" single-photon loss ($\kappa_1/\lambda < 2$) can induce phase-flip errors (in the basis above) that are not passively correctable (while keeping bit-flip errors passively correctable), while large single-photon loss ($\kappa_1/\lambda > 2$) can induce both phase-flip and bit-flip errors that are not passively correctable. Errors that cannot be corrected passively must be actively corrected, e.g. via redundantly encoding into ancilla qubits.

[S1] T. Prosen, New Journal of Physics **10**, 043026 (2008).
[S2] T. Prosen and T. H. Seligman, Journal of Physics A: Mathematical and Theoretical **43**, 392004 (2010).
[S3] V. V. Albert and L. Jiang, Phys. Rev. A **89**, 022118 (2014).
[S4] E. Knill, R. Laflamme, and L. Viola, Phys. Rev. Lett. **84**, 2525 (2000).
[S5] D. A. Lidar, I. L. Chuang, and K. B. Whaley, Phys. Rev. Lett. **81**, 2594 (1998).
[S6] V. V. Albert, B. Bradlyn, M. Fraas, and L. Jiang, Phys. Rev. X **6**, 041031 (2016).
[S7] M. Mirrahimi, Z. Leghtas, V. V. Albert, S. Touzard, R. J. Schoelkopf, L. Jiang, and M. H. Devoret, New Journal of Physics **16**, 045014 (2014).
[S8] R. Blume-Kohout, H. K. Ng, D. Poulin, and L. Viola, Phys. Rev. A **82**, 062306 (2010).